ORIGINAL RESEARCH PAPER

Fuel Cells DOI: 10.1002/fuce.200800152

Alumina Doped Ni/YSZ Anode Materials for Solid Oxide Fuel Cells

C. R. He[1], W. G. Wang[1]*

[1] Ningbo Institute of Material Technology and Engineering (NIMTE), Chinese Academy of Sciences, Ningbo 315201, PR China

Received November 6, 2008; accepted July 2, 2009

Abstract

The Al_2O_3–Ni–YSZ (Y_2O_3 stabilised ZrO_2) anode materials with 0–6 wt% Al_2O_3 were prepared by tape casting method after being ball-milled for 48 h. The influence of Al_2O_3 content on flexural strength, electrical conductivity, open porosity, relative density and thermal expansion coefficient (TEC) of Al_2O_3–Ni–YSZ anode was investigated. The introduction of Al_2O_3 significantly enhances the flexural strength of Al_2O_3–Ni–YSZ anode. The flexural strengths of 430 and 299 MPa are achieved for the specimen containing 0.25 wt% Al_2O_3 before and after reduction, respectively, while the flexural strengths are 201 and 237 MPa for the Ni–YSZ samples. The density decreases with increasing Al_2O_3 content and the open porosity increases correspondingly, after being sintered at 1350 °C for 4 h. The electrical conductivity at ambient temperature does not fall off when Al_2O_3 content is less than 1 wt%, but decreases rapidly when the content is above 3 wt% due to the formation of $NiAl_2O_4$. A maximum electrical conductivity of 1418 S cm^{-1} is obtained in the sample containing 0.5 wt% Al_2O_3. The TEC of the samples decreases with the introduction of Al_2O_3 in the temperature range of 20–850 °C.

Keywords: Alumina Doped Ni/YSZ Anode, Flexural Strength, Mechanical Properties, SOFC, TEC

1 Introduction

Solid oxide fuel cells (SOFCs) have attracted increasing attention in recent years because of their high energy conversion efficiency, low pollution and flexibility of fuels [1, 2]. In comparison with the electrolyte supported design, anode supported SOFC design is better suited for operation at lower temperatures because lesser ohmic loss and better interface contact can be realised, especially when composite electrodes are used to increase the density of triple phase boundaries (TPBs) [3–5].

At present, a cermet consisting of Ni metal and Y_2O_3 stabilised ZrO_2 (YSZ) is widely used as an anode material in SOFC. This material is preferred because of its good electronic conductivity, chemical and structural stability, catalytic properties and compatibility with other materials in SOFC [6]. The reliability of SOFC depends not only on the chemical and electrochemical stability of its components but also on the capability of the SOFC components to withstand mechanical stresses. During the assembly of stack and normal operation, the cermet anode should withstand mechanical loading to some extent to prevent the cell from cracking caused by various stresses. Therefore, the mechanical stability of anode support layer, in anode-supported SOFC design, is very important, especially for large scale applications.

Ceramics are brittle materials and many attempts have been made to increase their toughness by manipulating their microstructures. One technique is to introduce a second phase which has a thermal mismatch with the matrix, and hence the induced internal stress field can deflect or pin cracks. It is reported that a proper doping level of Al_2O_3 shows a beneficial effect on the sintering behavior as well as on the electrical and mechanical properties of YSZ electrolytes [7–9].

The YSZ phase in Ni–YSZ anode adjusts the thermal expansion coefficient (TEC) mismatch between YSZ and Ni, and as a framework, inhibits nickel coarsening at elevated temperatures [10, 11]. The purpose of this paper is to enhance the physical properties of Ni–YSZ anode material by doping alumina withoutreducing its electrical performance.

2 Experimental Procedures

The Al_2O_3–Ni–YSZ anode materials were produced from high purity (>99.99%) NiO, Al_2O_3 (about 10–20 nm) powders and commercial 3 mol% Y_2O_3 stabilised ZrO_2 (3YSZ, TOSOH

[*] *Corresponding author, wgwang@nimte.ac.cn*

Corp.). Green samples containing 44 wt% 3YSZ and 56 wt% NiO with 0–6 wt% Al_2O_3 of the total YSZ/NiO anode were prepared by tape casting method. To determine the samples' phase structure, X-ray diffraction analysis (XRD, Brucker D8 Advance, Germany) was performed at room temperature and the surface of the as-sintered samples were investigated using a field emission scanning electron microscope (FESEM), Hitachi S4800. The electrical conductivity was tested using a four-point probe fixture at ambient temperature. Rectangular specimens for the testing were cut from tapes and sintered at 1350 °C in air for 4 h and then reduced in H_2 at 850 °C for 2 h. The density and open porosity of sintered samples were determined by Archimedes method.

For flexural strength measurements, specimens of 4 mm × 0.4 mm × 36 mm were cut by laser and polished after being sintered at 1350 °C in air for 4 h and approximately half of the samples were reduced in H_2 at 850 °C for 2 h. The number of specimens was more than 12 in order to acquire average flexural strength, and the thickness of each specimen was determined by micrometer caliper in this paper. The flexural strength (σ_f) was measured using the three-point bending test and calculated by the following equation:

$$\sigma_f = 3PL/2bd^2$$

where σ_f is the flexural strength, P is the load, L is the span length, b is the width of the specimen and d is the thickness of the specimen. The specimens were tested using an Instron machine (Model 5567) according to ASTM test method C1161 with a cross-head speed of 0.3 mm min^{-1}. The TEC of Ni–YSZ anode with 0–6 wt% Al_2O_3 was determined by PCY-β TEC testing equipment (Xiangtan, China) in the temperature range from 20 to 850 °C.

3 Experimental Results and Discussions

3.1 XRD Patterns and SEM Photographs

Figure 1 shows the XRD patterns of the sintered $(Ni/YSZ)_{1-x}$ $(Al_2O_3)_x$ (x = 0.01, 0.02, 0.03, 0.04) specimens at 1350 °C for 4 h. The positions of XRD diffraction peaks for Al_2O_3-doped Ni/YSZ specimens remain unchanged, which suggests that the doping of Al_2O_3 cannot lead to phase transformation. However, when alumina content is more than 1 wt% of the Ni/YSZ solid, the diffraction peaks for Al_2NiO_4 are formed. Figure 2 is the SEM photograph of the reduced specimen with 1 wt% Al_2O_3. As shown in the figure, three different phases are visible: Ni phase, YSZ phase and a new nanosized phase on the boundaries of YSZ.

Figures 3 and 4 are the SEM micrograph and the EDS pattern of the specimen with 2 wt% Al_2O_3, respectively. In the SEM picture, four phases can be recognised: Ni phase, YSZ phase, a new nanosized phase on boundaries of YSZ and a new second-phase grown on the surface of nickel. The EDS microanalysis results of the whole area show strong X-ray peaks corresponding to Ni K line, Zr L line Al K and O K line, respectively. Thus, Al-rich phase exists in the samples with 1 and 2 wt% Al_2O_3. According to the XRD patterns, the two new phases observed in Figure 3 must be Al-rich phases. The spherical phase on the surface of nickel should be the Al_2NiO_4 phase which has huge ohmic resistance in compari-

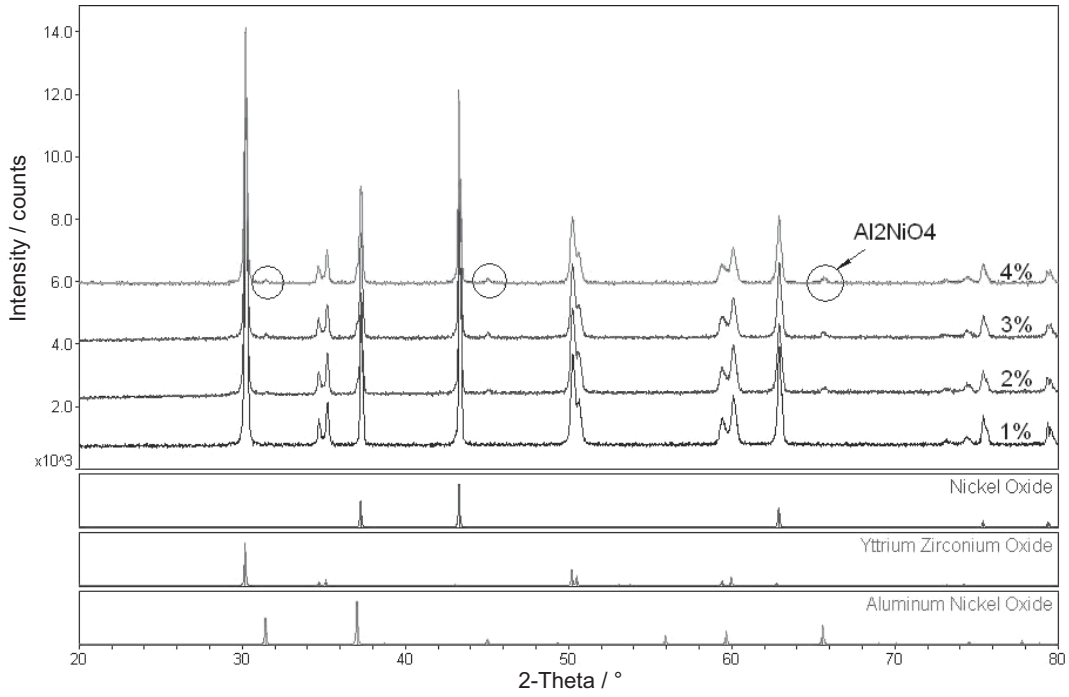

Fig. 1 XRD patterns of sintered $(Ni–YSZ)_{1-x}(Al_2O_3)_x$ (x = 0.01, 0.02, 0.03, 0.04).

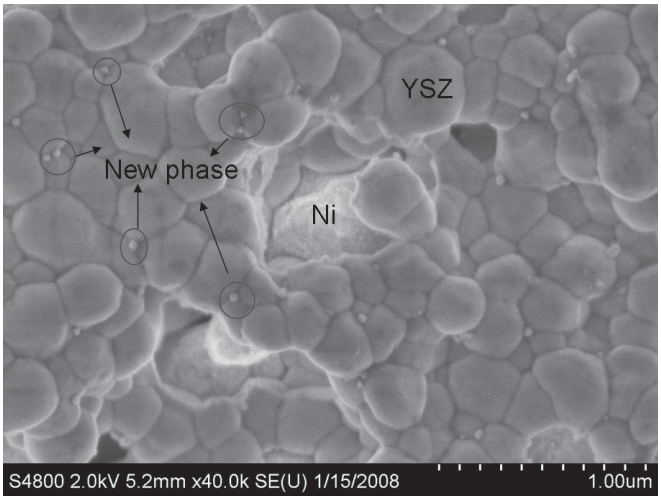

Fig. 2 SEM micrograph of sample with 1 wt% Al_2O_3.

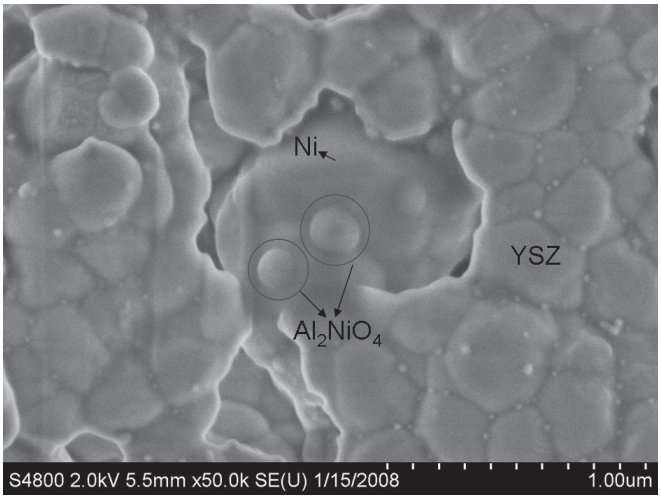

Fig. 3 SEM micrograph of sample with 2 wt% Al_2O_3.

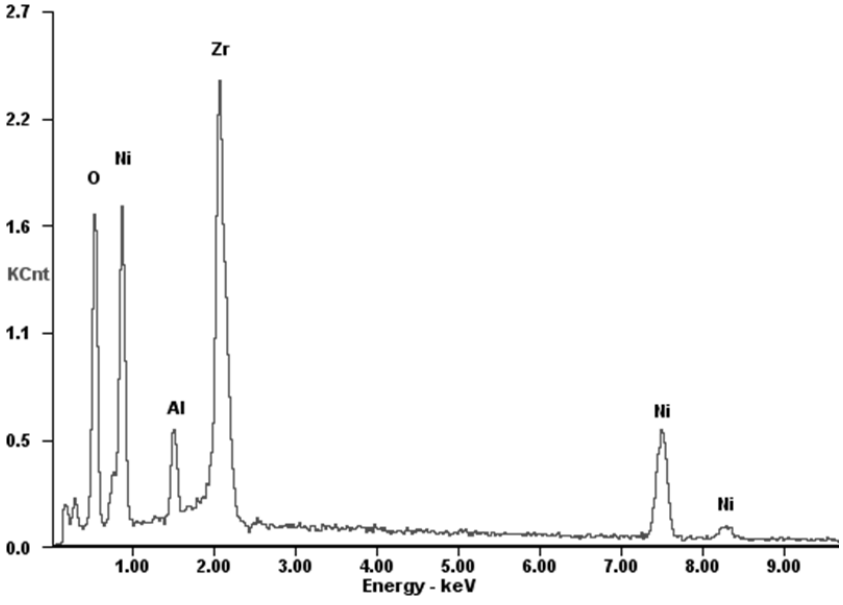

Fig. 4 EDS spectra of sample with 2 wt% Al_2O_3.

son with nickel phase. The nanosized phase on the boundaries of YSZ may be the Al_2O_3. From the XRD, EDS patterns and SEM photographs, it can be concluded that the amount of 1 wt% Al_2O_3 is too low to escape scanning of X-rays and same is true for the Al_2NiO_4 phase, which leads to lower electrical conductivity.

3.2 Electrical Conductivity

Figure 5 presents the electrical conductivity of the reduced samples as a function of Al_2O_3 content. It is shown that the electrical conductivity at ambient temperature decreases with increasing content of Al_2O_3 due to the formation of Al_2NiO_4 phase. The electrical conductivity is more than 1200 S cm^{-1} when the amount of Al_2O_3 is less than 1 wt% and there is no obvious evidence of the formation of Al_2NiO_4 phase in XRD patterns. The electrical conductivity of the sample with 2 wt% Al_2O_3 is more than 1000 S/cm^{-1}; however, when the Al_2O_3 content is over 4 wt%, the electrical conductivity abruptly decreases to less than 500 S cm^{-1}. Therefore, there is no obvious influence of alumina content on the electrical conductivity when alumina is less than 1 wt%. Moreover, the sample containing 0.5 wt% Al_2O_3 obtains the highest electrical conductivity of 1418 S cm^{-1} at ambient temperature.

3.3 Density and Open Porosity

Samples for density and open porosity testings were prepared by tape casting method without any pore formers, then sintered in air at 1350 °C for 4 h and half of the specimens were reduced in H_2 at 850 °C for 2 h. The density and open porosity, as a function of alumina content for Ni–YSZ–Al_2O_3 composites, are shown in Figures 6 and 7, respectively. It is shown that the sintered density increases with increasing Al_2O_3 content up to 0.25 wt% and decreases when the Al_2O_3 addition is over 0.25 wt%, both before and after reduction as shown in Figure 6. The density determined by Archimedes method is higher than the unloaded Ni/YSZ specimen when the amount of Al_2O_3 is less than 1 wt%. When the Al_2O_3 concentration is over 4 wt%, the sintered density of the loaded samples is lower than that of the unloaded specimen, and the density of specimen containing 4 wt% Al_2O_3 is the lowest one in this investigation. The open porosity results of the reduced samples show the opposite trend for the sintered density (Figure 7 and Table 1). The average open porosity is only 17.3% when the concentration of Al_2O_3 is up to 0.25 wt% and increases with the increasing alumina content when the concentration of Al_2O_3 is over 0.25 wt%. The mean open porosity of the specimen containing 4 wt% Al_2O_3 is 25.7%, the highest value in this work.

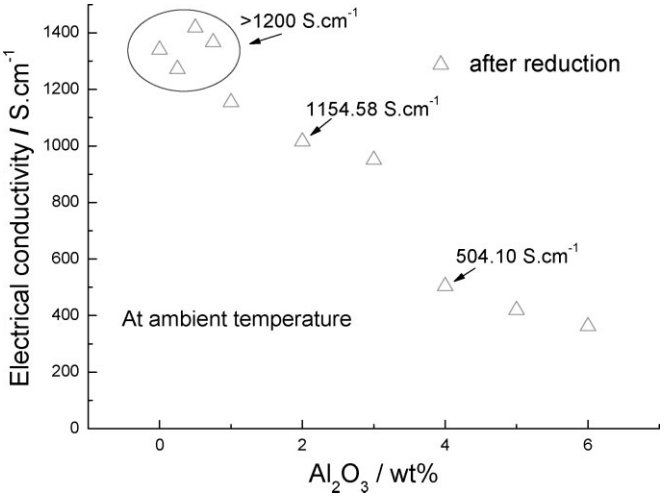

Fig. 5 The electrical conductivity as a function of Al_2O_3 content.

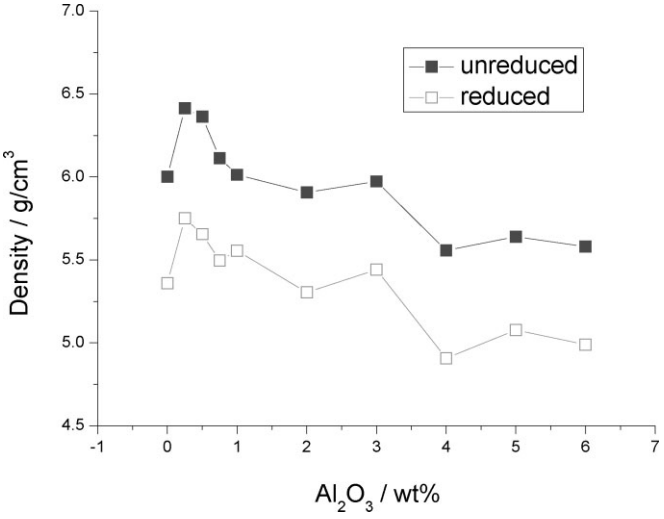

Fig. 6 The effect of Al_2O_3 content on density of Ni–YSZ–Al_2O_3 composites before and after reduction.

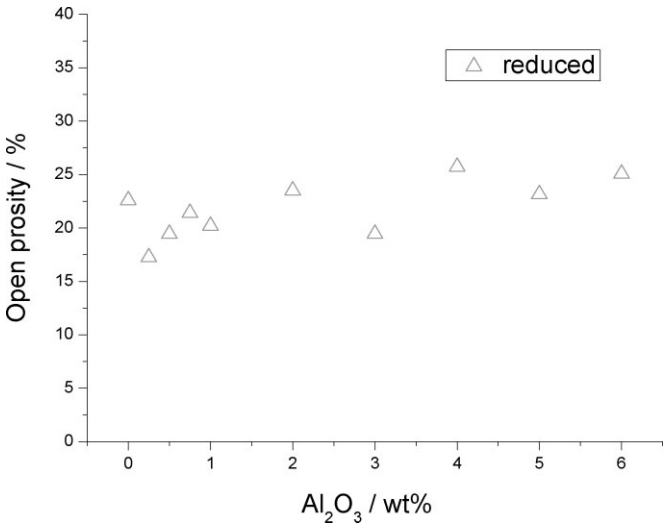

Fig. 7 The effect of Al_2O_3 content on open porosity of Ni–YSZ–Al_2O_3 composites reduced in H_2 at 850 °C for 2 h.

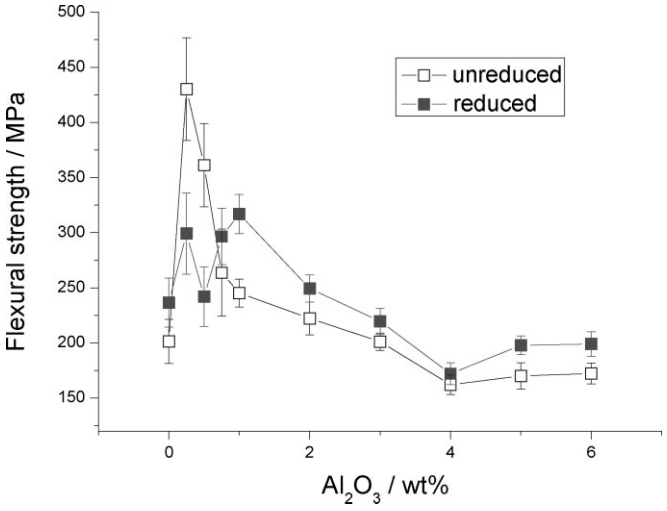

Fig. 8 The effect of Al_2O_3 content on flexural strength of the composites before and after reduction.

The doping of Al_2O_3 with the doping content below 1 wt% in the Ni/YSZ can promote the sintering of Ni/YSZ anode due to the small size effect of Al^{3+} [12], but the increasing number of additions readily lead to the precipitation of Al-rich phase at the grain boundaries and the formation of Al_2NiO_4 phase as discussed above. The pinning effect of the Al-rich phase at grain boundaries may inhibit the growth of grains, so the sintered density decreases while the open porosity increases.

3.4 Flexural Strength

Anode supported SOFC design, as the name says, also dominates the mechanical strength of the cell. The flexural strength as a function of the Al_2O_3 content is shown in Figure 8. It can be seen that the addition of Al_2O_3 enhances the flexural strength of Ni–YSZ–Al_2O_3 anode when the amount of alumina is less than 3 wt% whereas the flexural strength becomes lower than the unloaded sample when the alumina content is over 3 wt%. This may be due to the formation of Al_2NiO_4 phase. The flexural strength increases from 201.40 to 430.22 MPa with doping 0.25 wt% Al_2O_3 before reduction and from 236.62 to 316.90 MPa with doping 1 wt% Al_2O_3 after reduction. The data in details is shown in Table 2. The

Table 1 Open porosity of the reduced samples (open porosity was determined by Archimedes method <average value> ± <standard deviation>).

Al_2O_3 content (wt%)	0	0.25	0.5	0.75	1	2	3	4	5	6
Open porosity (%)	22.6 ± 1.6	17.3 ± 2.5	19.5 ± 0.9	21.4 ± 1.7	20.2 ± 1.1	23.5 ± 0.6	19.5 ± 0.4	25.7 ± 0.1	23.2 ± 1.1	25.1 ± 0.9

Table 2 Flexural strength of samples before and after reduction.

Sample	Al_2O_3 (wt%)	Average flexural strength (MPa; unreduced)	Standard deviation	Average flexural strength (MPa; reduced)	Standard deviation
1	0	201.40	19.98	236.62	22.32
2	0.25	430.22	46.51	299.12	36.70
3	0.5	361.19	37.68	242.01	27.20
4	0.75	263.62	39.50	296.54	25.55
5	1	245.26	12.57	316.90	17.91
6	2	222.24	14.84	249.43	12.33
7	3	201.11	7.86	219.57	11.87
8	4	162.04	8.85	172.02	9.90
9	5	170.04	12.00	197.85	8.52
10	6	172.26	9.53	198.97	11.16

specimen containing 4 wt% Al_2O_3 has the lowest flexural strength in this paper. The flexural strength of the reduced samples exhibits no significant enhancement in either the first or in the repeated experiment when the amount of alumina is up to 0.5 wt%, for unknown reasons.

Figure 9 shows the Weibull distribution of flexural strength of the sample with 0.25 wt% Al_2O_3. The sample shows an average flexural strength of around 430.22 ± 46.51 MPa with a minimum strength of 350.40 MPa before reduction and around 299.12 ± 36.70 MPa with a minimum strength of 239.55 MPa after reduction.

The improvement in the flexural strength can be attributed to the following reasons. Firstly, the high elastic modulus of Al_2O_3 induces a remarkable shielding effect during crack propagation by crack-bridging and crack-deflection mechanisms [6]. Most ceramics in commercial use are polycrystalline. Each grain generally has a crystal orientation, which is different from adjacent grains. A crack passing through a polycrystalline ceramic does not follow a smooth planar path. It follows grain boundaries around some grains and fractures other grains. This results in greater fracture energy and greater flexural strength. Secondly, the remarkable mismatching of lattice parameters [13] and TECs between matrix and second phase particles leads to compressive stresses, which deflect cracks and thus improve mechanical properties. Thirdly, the second phase particles have a strengthening effect due to crack deflection and thereby partially contribute to enhance the flexural strength of YSZ–Al_2O_3 composite [14].

The formation of Al_2NiO_4 phase lowers the content of ductile Ni and high-elastic-modulus Al_2O_3 phase. Since the effect of Al_2NiO_4 phase becomes larger than the effect of Al_2O_3 phase when the Al_2O_3 addition is more than 3 wt%, the flexural strength of Al_2O_3-loading specimens is lower than the unloaded sample.

3.5 TEC

Since nickel has higher TEC than YSZ, there are concerns about thermal expansion mismatch between the anode and the electrolyte. A significant mismatch in TEC of SOFC components may result in large stresses, causing cracks during fabrication and operation. Columned samples were pressed with about 200 MPa for 5 min from ball-milled NiO–YSZ–Al_2O_3 composite, and then sintered at 1350 °C for 4 h in air for the TEC testing. In this paper, as demonstrated in Figure 10, the TEC of the samples decreases with the introduction of Al_2O_3 at the temperature range of 20–850 °C. This is mainly due to the lower TEC of Al_2O_3 (8.8×10^{-6} K^{-1}) and the formation of Al_2NiO_4 phase (which lowers the content of ductile Nickel phase).

4 Conclusions

The electrical conductivity, open porosity, relative density, flexural strength and TEC of Ni–YSZ–Al_2O_3 anode with 0–6

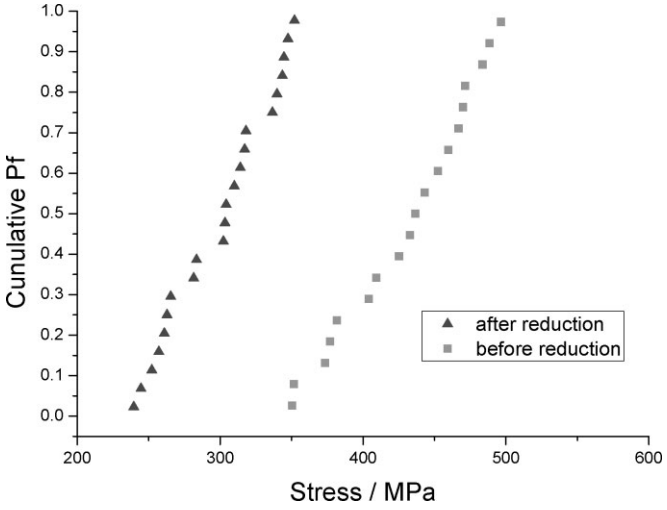

Fig. 9 Weibull distribution of flexural strength of the sample with 0.25 wt% Al_2O_3.

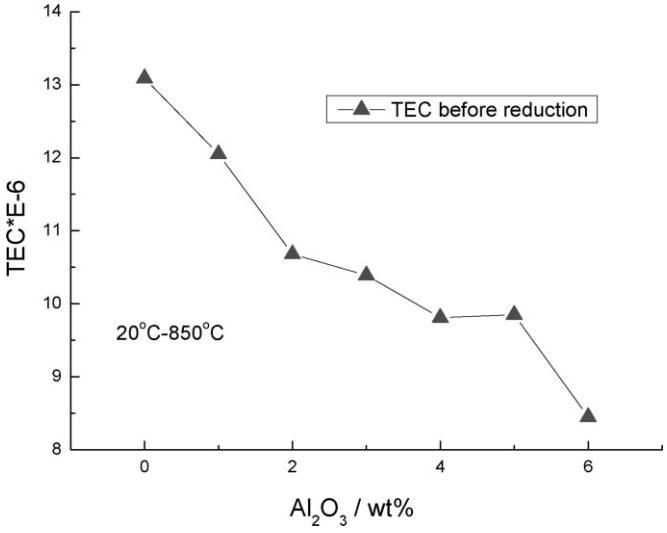

Fig. 10 The TEC as a function of Al_2O_3 content.

wt% Al_2O_3 were investigated. There is no obvious influence on the electrical conductivity when alumina content is less than 1 wt% and the sample containing 0.5 wt% Al_2O_3 achieves the highest electrical conductivity of about 1418 S cm^{-1} at ambient temperature. The density of the samples decreases with the increasing Al_2O_3 content, and the open porosity increases correspondingly. It can be seen that the addition of Al_2O_3 significantly enhances the flexural strength of Ni–YSZ–Al_2O_3 anode when the amount of alumina is less than 3 wt%, but the flexural strength is lower than the unloaded sample when the alumina content is over 3 wt% due to the formation of Al_2NiO_4 phase. The flexural strength is 430 and 299 MPa for the specimen containing 0.25 wt% Al_2O_3 before and after reduction, respectively, while the flexural strength is 201 and 237 MPa for the Ni–YSZ sample. The lower TEC of Al_2O_3 and the formation of Al_2NiO_4 phase lead to the decrease of TEC with increasing content of Al_2O_3.

Acknowledgements

This work was financially supported by the National High-Tech Research and Development Program of China (863 Program, grant no. 2007AA05Z140), the Qian Jiang Ren Cai Program (grant no. 2008R10003) and the Chinese Academy of Sciences.

References

[1] N. Q. Minh, *J. Am. Ceram. Soc.* **1993**, *76*, 563.
[2] M. Dokiya, *Solid State Ionics* **2002**, *152/153*, 383.
[3] F. Zhao, A. V. Virkar, *J. Power Sources* **2005**, *141*, 79.
[4] A. C. Müller, D. Herbstritt, E. I. Tiffée, *Solid State Ionics* **2002**, *152–153*, 537.
[5] Z. R. Wang, J. Q. Qian, S. R. Wang, J. D. Cao, T. L. Wen, *Solid State Ionics* **2008**, *179*, 1593.
[6] M. Radovic, E. Lara-Curzio, *Acta Mater.* **2004**, *52*, 5747.
[7] S. Tekeli, *Mater. Des.* **2006**, *27*, 230.
[8] J. S. Lee, K. H. Choi, B. K. Ryu, B. C. Shin, I. S. Kim, *Ceram. Int.* **2004**, *30*, 807.
[9] H. Xu, H. Yan, Z. Chen, *Mater. Sci. Eng.* **2007**, *A447*, 222.
[10] S. D. Kim, H. Moon, S. H. Hyun, J. Moon, J. Kim, H. W. Lee, *Solid State Ionics* **2007**, *178*, 1304.
[11] S. K. Pratihar, A. D. Sharma, R. N. Basu, H. S. Maiti, *J. Power Sources* **2004**, *129*, 138.
[12] T. S. Zhang, J. Ma, S. H. Chan, J. A. Kilner, *Solid State Ionics* **2005**, *176*, 377.
[13] A. J. Feighery, J. T. S. Irvine, *Solid State Ionics* **1999**, *121*, 209.
[14] K. Oe, K. Kikkawa, A. Kishimoto, et al., Y. Kanamura, H. Yanagida, *Solid State Ionics* **1996**, *91*, 131.

